

Cryogenic low-noise amplifiers of low power dissipation for space terahertz astronomy

Jie Liu(刘洁), Dong Liu(刘冬), Kun Zhang(张坤), Ming Yao(姚明), Jun-Da Jin(金骏达), Qi-Jun Yao(姚骑均), Jing Li(李婧), and Sheng-Cai Shi(史生才)

Citation: Chin. Phys. B, 2026, 35 (**4**): 048502. DOI: 10.1088/1674-1056/ae0019
http://cpb.iphy.ac.cn; http://iopscience.iop.org/cpb

What follows is a list of articles you may be interested in

Dynamic electrostatic-discharge path investigation relied on different impact energies in metal-oxide-semiconductor circuits

Tian-Tian Xie(谢田田), Jun Wang(王俊), Fei-Bo Du(杜飞波), Yang Yu(郁扬), Yan-Fei Cai(蔡燕飞), Er-Yuan Feng(冯二媛), Fei Hou(侯飞), and Zhi-Wei Liu(刘志伟)

Chin. Phys. B, 2023, 32 (**4**): 048501. DOI: 10.1088/1674-1056/ac9607

C band microwave damage characteristics of pseudomorphic high electron mobility transistor

Qi-Wei Li(李奇威), Jing Sun(孙静), Fu-Xing Li(李福星), Chang-Chun Chai(柴常春), Jun Ding(丁君), and Jin-Yong Fang(方进勇)

Chin. Phys. B, 2021, 30 (**9**): 098502. DOI: 10.1088/1674-1056/abf135

Universal memory based on phase-change materials: From phase-change random access memory to optoelectronic hybrid storage

Bo Liu(刘波), Tao Wei(魏涛), Jing Hu(胡敬), Wanfei Li(李宛飞), Yun Ling(凌云), Qianqian Liu(刘倩倩), Miao Cheng(程淼), and Zhitang Song(宋志棠)

Chin. Phys. B, 2021, 30 (**5**): 058504. DOI: 10.1088/1674-1056/abeedf

Vertical polarization-induced doping InN/InGaN heterojunction tunnel FET with hetero T-shaped gate

Yuan-Hao He(何元浩), Wei Mao(毛维), Ming Du(杜鸣), Zi-Ling Peng(彭紫玲), Hai-Yong Wang(王海永), Xue-Feng Zheng(郑雪峰), Chong Wang(王冲), Jin-Cheng Zhang(张进成), and Yue Hao(郝跃)

Chin. Phys. B, 2021, 30 (**5**): 058501. DOI: 10.1088/1674-1056/abd73f

In-memory computing to break the memory wall

Xiaohe Huang(黄晓合), Chunsen Liu(刘春森), Yu-Gang Jiang(姜育刚), Peng Zhou(周鹏)

Chin. Phys. B, 2020, 29 (**7**): 078504. DOI: 10.1088/1674-1056/ab90e7

Cryogenic low-noise amplifiers of low power dissipation for space terahertz astronomy

Jie Liu(刘洁), Dong Liu(刘冬), Kun Zhang(张坤), Ming Yao(姚明),
Jun-Da Jin(金骏达), Qi-Jun Yao(姚骑均), Jing Li(李婧), and Sheng-Cai Shi(史生才)†

Purple Mountain Observatory, Chinese Academy of Sciences, Nanjing 210023, *China*

(Received 2 July 2025; revised manuscript received 13 August 2025; accepted manuscript online 28 August 2025)

Cryogenic low-noise amplifiers (CLNAs) are of particular interest for applications such as radio astronomy and quantum information science. Here we report on the design and characterization of low-power-dissipation wideband CLNAs for a terahertz spectrometer onboard China's Space Station Telescope (CSST). A simple small-signal and noise model is established based on the DC and RF characteristics of SiGe heterojunction-bipolar-transistors (HBTs) adopted for this development. The developed SiGe HBT CLNAs at 4 K demonstrate an average noise temperature of 4.5 K and a gain of exceeding 35 dB in the frequency range of 0.1 GHz–1.1 GHz. With the power dissipation as low as 3 mW, the average noise temperature is still as low as 6.8 K. The combination of low power dissipation and low noise temperature is rather beneficial to applications in space instruments and complex systems.

Keywords: SiGe heterojunction-bipolar-transistor (HBT), low noise amplifier, low power

PACS: 85.30.Pq, 84.30.Le, 95.55.Jz

DOI: 10.1088/1674-1056/ae0019 **CSTR:** 32038.14.CPB.ae0019

1. Introduction

The terahertz (THz) regime, loosely defined as 0.1 THz–10 THz, is a unique frequency band in observing cold and dark universe, which is invisible in the optical/near-infrared regime.[1] The Purple Mountain Observatory of Chinese Academy of Sciences is leading the development of a terahertz spectrometer (also known as High-Sensitivity Superconducting Detection Module, HSTDM[2]) onboard China's Space Station Telescope (CSST) as one of five CSST's scientific instruments. The THz spectrometer mainly observes terahertz spectral lines in the frequency range of 0.41 THz–0.51 THz (*e.g.*, atomic carbon CI line at 0.492 THz). Its receiver frontend is mainly composed of two NbN-based superconductor-insulator-superconductor (SIS) mixers[3] and two following intermediate-frequency (IF, 0.1 GHz–1.1 GHz) low-noise amplifiers, which are cooled down to approximately 8 K by a two-stage pulse-tube cryocooler for space applications.[4] As the cooling capacity of the two-stage pulse-tube cryocooler is limited, the adopted CLNAs should have power dissipation of no more than 5 mW, yet with a noise temperature below 10 K.

As is well known, cryogenic InP-based high-electron-mobility-transistors (HEMTs) have been widely used in radio astronomical receivers because of their state-of-the-art noise performance.[5] However, their operating frequency is typically above 1 GHz and power dissipation is above 5 mW. Recent studies demonstrate that SiGe-based HBTs perform well at frequencies as low as 0.1 GHz and at temperatures down to 4 K.[6–8] Furthermore, HBTs appear superior to HEMTs in power dissipation.[6,9] SiGe-based HBT CLNAs are thus of particular interest for space applications and large complex systems such as multibeam/phased-array receivers and quantum computers. We chose SiGe-based HBTs to develop 0.1 GHz–1.1 GHz CLNAs for our THz spectrometer. Through this development, we firstly build a small-signal and noise model at low temperatures and then study the noise and gain dependence upon DC power dissipation at different temperatures.

2. A combined small-signal and noise model

Small-signal and noise models are usually established separately in designing low-noise amplifiers. For HBTs, a combined small-signal and noise model has been proposed,[10,11] as shown in Fig. 1. It can be seen clearly that there are mainly thermal noises from uncorrelated base/collector/emitter physical resistances (i.e., $v_{n,b}$, $v_{n,c}$, and $v_{n,e}$) and partially correlated base and collector shot noises (i.e., $i_{n,b}$ and $i_{n,c}$).[12] Note that when the operating frequency is less than $f_T/3$, (f_T is transistor's cutoff frequency) this correlation is rather limited and can be ignored.[13] As we adopt packaged transistors like industry standard SOT343 in our design, an emitter parasitic inductor L_e is introduced to take account of the packing effect that is considerable especially for a large relative bandwidth like 0.1 GHz–1.1 GHz. The parasitic inductance L_e is primarily responsible for the decrease in amplifier gain with increasing operating frequency. The small-signal and noise parameters can be extracted from the

†Corresponding author. E-mail: scshi@pmo.ac.cn

© 2026 Chinese Physical Society and IOP Publishing Ltd. All rights, including for text and data mining, AI training, and similar technologies, are reserved.

measured RF and DC characteristics at different temperatures, respectively.

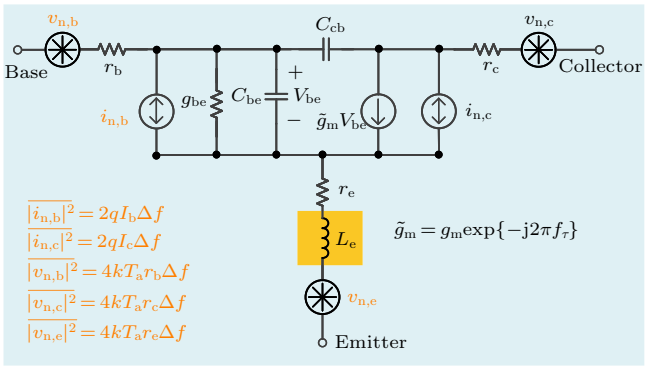


Fig. 1. A combined small-signal and noise model for the design of cryogenic HBT amplifiers, with the emitter parasitic inductor L_e added for packaged HBT transistors.

Once the critical model parameters have been defined, the radio frequency performance of the amplifier can be simulated using the small signal and noise model discussed previously. It is worth noting that some parameters exhibit less sensitivity to ambient temperature fluctuations. Consequently, these parameters can be determined from the DC and RF characteristics measured at room temperature. They include the base resistance r_b, collector resistance r_c, emitter resistance r_e, and the parasitic collector-base capacitance C_{cb}.

Before determining all the model parameters, we estimated the minimal noise temperature T_{min} associated with the operating temperature and bias current based on the transistor's DC characteristics.[9,10] It can be evaluated with a simpler expression as

$$T_{min} \approx T_a \frac{n_{cx}}{\sqrt{\beta}}, \tag{1}$$

where T_a is the ambient temperature, $\beta = I_c/I_b$ is the current gain, $n_{cx} = I_c/(G_m V_T)$ is the extrinsic collector current ideality factor, $G_m = dI_c/dV_{be}$ is the extrinsic transconductance, I_c is the collector current, $V_T = kT_a/q$ is the thermal voltage, k is Boltzmann constant, and q is the magnitude of charge of an electron. This simplified noise-temperature expression is valid at frequencies that are much lower than the transistor's cutoff frequency. Obviously, the current gain β and transconductance g_m, which are temperature-dependent, can be characterized through the DC measurements of the transistor at temperatures from 290 K to 4 K.

For BFP842ESD SiGe transistors, figure 2 illustrates the dependence of the current gain β and extrinsic transconductance G_m on the collector current at 290 K and 4 K. Based on the trade-off between gain and noise, an optimal collector current of 4 mA was selected. At this bias point, the temperature-dependent behaviors of β and G_m are plotted in Fig. 3, with additional details provided in Table 1. The sharp increase of the two key parameters at cryogenic temperatures leads to a significant reduction in the noise contribution of the transistors. Based on the measured values of the transistor current gain β and transconductance G_m at different temperatures,

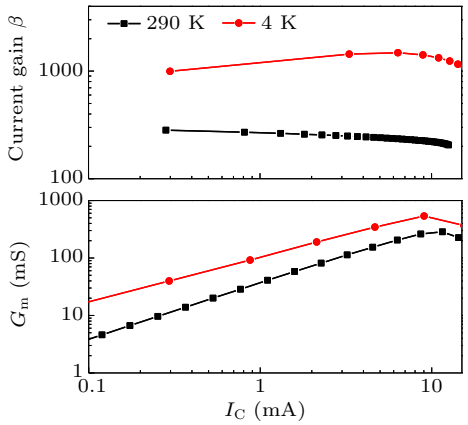


Fig. 2. Measured current gain β and extrinsic transconductance G_m as a function of collector current at 290 K and 4 K.

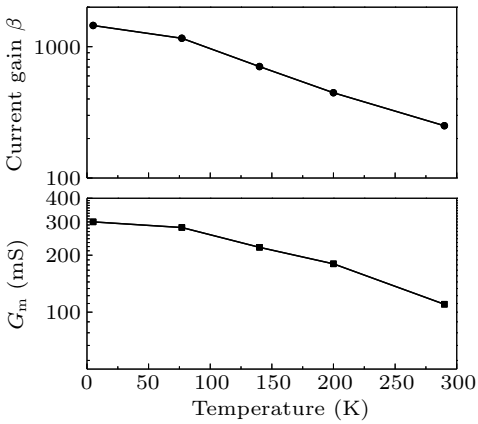


Fig. 3. Measured current gain β and extrinsic transconductance G_m as a function of ambient temperature at a collector current of 4 mA.

Table 1. Current gain β and extrinsic transconductance G_m for BFP842ESD at 290 K and 4 K at a collector current of 4 mA.

Device type	Ambient temperature (K)	β	G_m (mS)
BFP842ESD	290	250	120
	4	1450	300

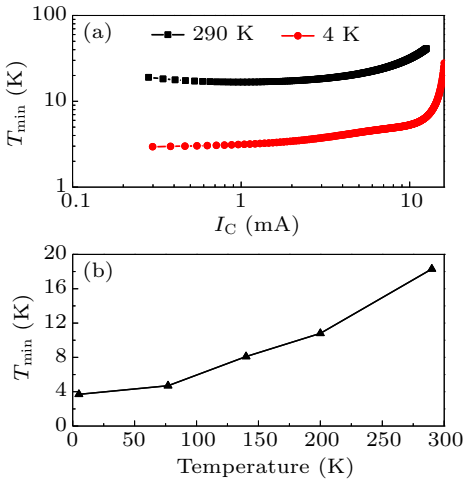


Fig. 4. Calculated T_{min} as functions of collector current (a) and ambient temperature (b).

the minimum noise temperature $T_{\min}$ was calculated, as depicted in Fig. 4. It can be clearly seen that this type of transistor exhibits excellent noise characteristics even at low collector currents, thereby making it suitable for the development of our 0.1–1.1 CLNAs particularly with low power dissipation.

After evaluating the transistors' cryogenic noise characteristics, we can select some transistors suitable for cryogenic applications and then extract small-signal model parameters. An open-collector method was utilized to determine the emitter resistance r_e. By setting the collector current to zero, the collector–emitter voltage V_{ce} was characterized as a function of the applied base current I_b. The value of r_e was then derived according to $r_e = \mathrm{d}V_c/\mathrm{d}I_b$. To obtain the collector resistance r_c, the DC source was configured in current–source mode, enabling precise control over the current I_c. Firstly, the collector voltage V_c was measured as a function of the base current I_b under a fixed I_c. Secondly, the relationship between V_c and I_c was established under a fixed base current I_b. It should be noted that calibrating the resistance of the DC test line was essential for this measurement. The value of r_c can be obtained by

$$r_c = \frac{\mathrm{d}V_c}{\mathrm{d}I_c} - \frac{\mathrm{d}V_c}{\mathrm{d}I_b} - r_p, \tag{2}$$

where r_p is the resistance of the DC test line. As for r_b, we can assume $r_b \approx r_c$, since the noise of the transistors is mainly the shot noise caused by the PN junction current at the ambient temperature close to absolute zero. The base-emitter junction admittance g_{be} defined as $g_{be} = \mathrm{d}V_b/\mathrm{d}I_b$, can also be extracted through DC measurement. To determine the baseemitter junction capacitance C_{be} and the collectorbase parasitic capacitance C_{cb}, the through-reflect-line (TRL) de-embedding calibrations were carried out for the measurement of S parameters at low temperatures. Note that for the extraction of the collector-base capacitance C_{cb}, we measured the S parameters under off-bias conditions, ensuring that the junction was reverse-biased. In this case, both the transconductance g_m and the base-emitter admittance g_{be} are almost zero, leaving only the parasitic capacitance of the transistor. Subsequently, the S-parameters of the transistor were converted into Y-parameters to determine the value of C_{cb}, which is given by

$$C_{cb} = -\frac{\mathrm{Im}\{Y_{12}\}}{\omega}. \tag{3}$$

The base-emitter capacitance C_{be}, which is dependent on the transistor's bias, can be determined in terms of the active bias S-parameters. Firstly, the S-parameters are converted into Z-parameters to eliminate the contributions of resistances r_b, r_c, and r_e. Secondly, the Z-parameters are transformed into Y-parameters from which C_{be} is extracted using the following equation:

$$C_{be} = -\frac{1}{\omega\,\mathrm{Im}\{1/Y_{11}\}} - C_{cb}. \tag{4}$$

At this point, two key parameters remain to be determined: the transconductance g_m and the emitter parasitic inductor L_e. The relationship between the external transconductance G_m and the intrinsic transconductance g_m is expressed as $G_m = g_m/(1 + g_m r_e)$. We can have $g_m \approx G_m$ when the emitter resistance r_e is small. The emitter parasitic inductor L_e can be determined by fitting the cryogenic forward transmission coefficient S_{21} of the amplifier circuit.

The small-signal model for the BFP842ESD transistor was established through the parameter extraction process described above, as listed in Table 2. With this model, its cryogenic scattering parameters were simulated. For the evaluation of the noise characteristics of the transistor, the two shot noises were calculated based on a base bias current $I_b = 2$ μA and a collector current $I_c = 4$ mA, respectively. The thermal noise contributions from the three resistive elements at ambient temperature T_a were calculated straightforwardly. This approach enabled an accurate estimation of both noise and gain characteristics, thereby facilitating the design and optimization of cryogenic low noise amplifiers. The comparative analysis of the simulated and measured results, with respect to the amplifier's gain and noise temperature, is presented in Section 4.

Table 2. Extracted parameters of the cryogenic smallsignal model of BFP842ESD.

Parameter	Value (Ω)	Parameter	Value
r_b	1.35	C_{cb}	70 fF
r_c	1.35	C_{be}	0.7 pF
r_e	0.13	g_m	300 mS
g_{be}	6e5	L_e	0.6 nH

3. Design of 0.1 GHz–1.1 GHz CLNAs

Based on the combined small-signal and noise model for the BFP842ESD transistor, a two-stage cryogenic amplifier operating from 0.1 GHz to 1.1 GHz was designed. The circuit schematic and the assembled discrete amplifier are illustrated in Fig. 5. To enhance the input impedance matching, gain flatness and stability, resistive negative feedback was implemented between the collector and emitter. It is well known that at room temperature the resistive feedback is generally considered to be an impractical option due to the increased thermal noise from the feedback resistance R_f. As the feedback resistance is cooled from 290 K to 4 K, however, its thermal noise reduces by a factor of 72. In addition, for $\beta/R_f \ll g_m/2$, the thermal noise introduced by the feedback resistance can be ignored.[14] Consequently, adding a high value feedback resistance for impedance matching does not adversely affect the noise performance of the amplifier. In our design, the use of RF-glass at the input and output ports provides superior stability under extreme thermal and mechanical conditions. Additionally, a small series resistor is introduced between amplifier stages, increasing the stability factor (K-factor) from 2.5 to 3.8

and thereby providing a larger stability margin while mitigating potential oscillations due to device aging. Furthermore, several bypass capacitors of 470 pF were placed near the transistor, while a larger capacitance of 0.1 μF was connected in parallel at the DC bias port to stabilize the transistor's bias.

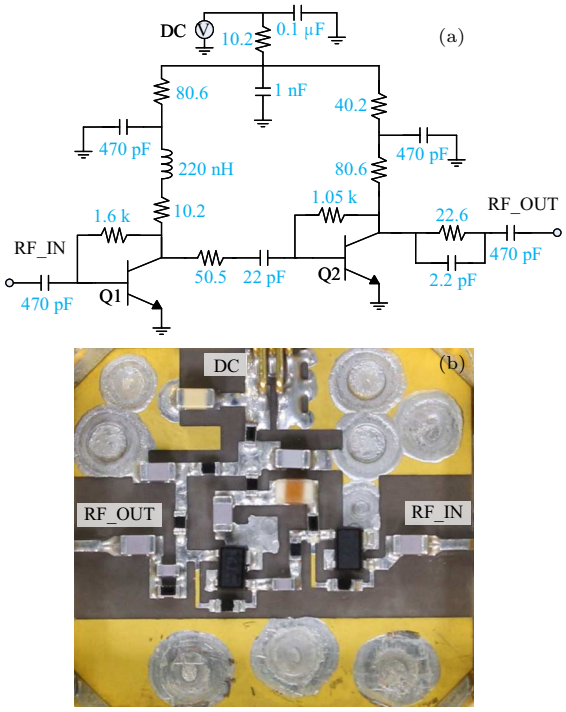


Fig. 5. (a) Schematic diagram of two-stage low noise amplifier, with the unit of the resistance values is Ω. (b) Assembled discrete amplifier with the sizes are 18 mm × 16.5 mm.

The microstrip lines of the amplifier were fabricated on a substrate Rogers 5880 with a thickness of 0.127 mm. This choice of thin dielectric material improves the isolation between the input and output ports of the circuit. It is worth noting that the transistors are mounted close to the via holes to minimize parasitic inductance and capacitance, which can significantly impact the amplifier stability at cryogenic temperatures. Furthermore, the cavity of the amplifier was carefully optimized through an isolated design of the DC and RF paths. This approach effectively suppresses potential resonances within the cavity, ensuring stable operation across the specified frequency range.

4. Measurement and analysis

The noise temperature and gain of the 0.1 GHz–1.1 GHz low-noise amplifier were measured inside a 4-K cryostat. The cryogenic noise measurements were performed using the cold attenuator method with an estimated noise-temperature accuracy of ±1 K.[15,16] The measured and simulated gain and noise temperature of the amplifier at 4 K are shown in Fig. 6. It can be clearly seen that both the measured gain and noise temperature agree well with the simulation ones, validating the approximate modeling approach used for the design. As you can see, the gain curve without the parasitic inductance L_e is quite different from that with L_e. To mitigate the gain degradation at higher frequencies, an equalization circuit has been implemented in the IF chain, leading to a substantial improvement in the spectral characteristics of the IF output. At the ambient temperature of 4 K, the optimal noise temperature occurs at a collector voltage of 1.6 V and a current of 8 mA. Under this condition, the average noise temperature across the frequency range of 0.1 GHz–1.1 GHz is 4.5 K, with a minimum value of 3.7 K at 0.16 GHz. The amplifier has a gain exceeding 35 dB throughout the entire operating frequency range. Additionally, the cryogenic amplifier's input and output voltage standing wave ratio (VSWR) values are both below 2, as shown in Fig. 7.

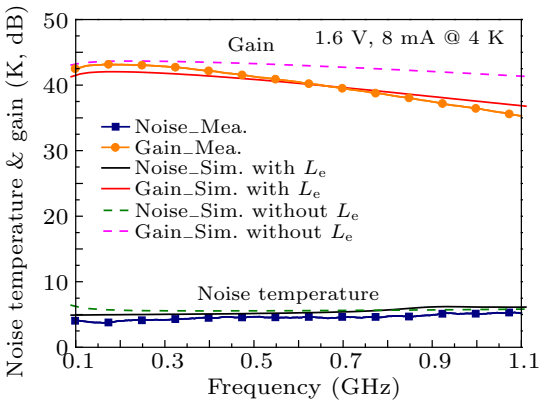


Fig. 6. Measured and simulated gain and noise temperature of the amplifier at 4 K as a function of frequency.

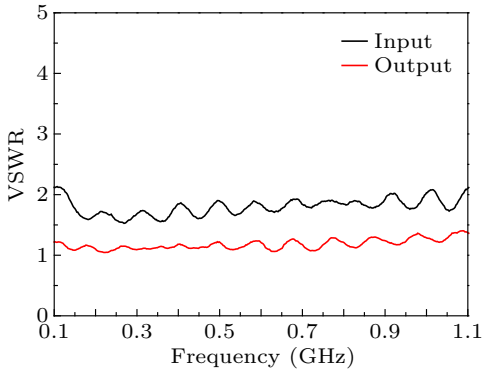


Fig. 7. Measured input and output VSWR of the amplifier at 4 K as a function of frequency.

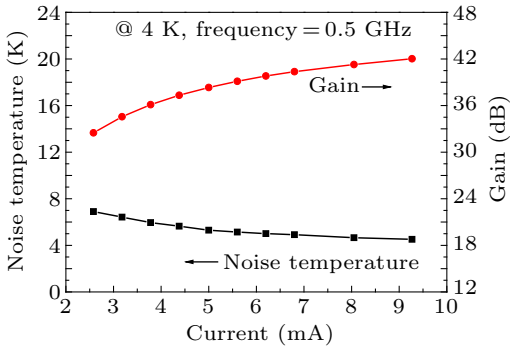


Fig. 8. Measured gain and noise temperature of the amplifier as a function of collector current at 4 K.

Figure 8 further demonstrates the dependence of the gain and noise temperature on the collector current at 0.5 GHz. Obviously, both the gain and noise temperature are insensitive to the collector current. Note that at a collector current of 2.6 mA, corresponding to a power dissipation of only 3 mW, the amplifier still demonstrates a gain greater than 32 dB and an average noise temperature of 6.8 K.

The amplifier underwent comprehensive environmental testing, including mechanical, thermal cycling, thermal vacuum, high-temperature life, and irradiation testing. As shown in Fig. 9, the amplifier's gain and noise temperature remain unchanged, demonstrating its robustness for space applications.

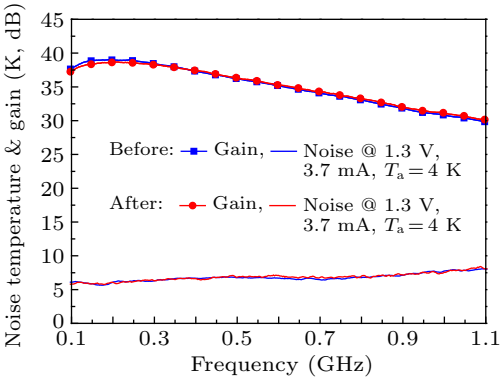


Fig. 9. Comparisons of the measured gain and noise temperature of the amplifier at 4 K before and after environmental testing.

A comparison of the amplifier's performance against recently published state-of-the-art SiGe cryogenic low-noise amplifiers is summarized in Table 3. The proposed amplifier demonstrates a combination of low noise temperature, high gain, and low power consumption, highlighting its suitability for space applications.

Table 3. Performance comparisons of SiGe cryogenic low noise amplifiers.

Reference	Frequency (GHz)	T_e (Avg) (K)	P_{DC} (mW)	Gain (dB)	T_a (K)
[17]	0.1–5	5	20	30	15
[18]	0.3–3	2.8	32	22	16
[19]	0.4–1.2	3.3	6.6	30	16
This work	0.1–1.1	4.5	12	35	4
*This work	0.1–1.1	6.8	3	32	4

*Operated at low power dissipation.

5. Conclusion and perspectives

A 0.1 GHz–1.1 GHz cryogenic low-noise amplifier (CLNA) has been developed for the terahertz spectrometer onboard China's Space Station Telescope (CSST). A combined small-signal and noise model was proposed to facilitate the amplifier design. Utilizing HBT transistors, this CLNA achieves good noise performance with low power dissipation. At a power dissipation of merely 3 mW, it exhibits an excellent average noise temperature of 6.8 K while maintaining a gain of over 32 dB. CLNAs of this kind, with low power dissipation and yet low noise temperature, should be of particular interest to space applications and complex systems.

Acknowledgements

Project supported in part by the National Key Research and Development Program of China (Grant Nos. 2023YFA1608201 and 2023YFF0722301), the Projects of International Cooperation and Exchanges, the National Natural Science Foundation of China (Grant No. 12020101002), and the Program of the Chinese Academy of Sciences (Grant No. PTYQ2024BJ0010).

References

[1] Li J, Deng X J, Li Y M, Hu J, Miao W, Lin C X, Jiang J and Shi S C 2025 *Research* **8** 0586
[2] Zhang K, Yao M, Liu D, Liu B L, Li J, Yao Q J and Shi S C 2023 *J. Infrared Millim. Waves* **42** 188
[3] Li J, Masanori Takeda, Wang Z, Shi S C and Yang J 2008 *Appl. Phys. Lett.* **92** 222504
[4] Quan J, Liu Y J, Liu D, Zhang K, Liang J T, Li J, Yao Q J and Shi S C 2014 *Chin. Sci. Bull.* **59** 3490
[5] Schleeh J, Rodilla H, Wadefalk N, Nilsson P Å and Grahn J 2014 *Solid-State Electronics* **91** 74
[6] Montazeri S, Grimes P K, Edward Tong C Y and Bardin J C 2016 *IEEE Trans. THz Sci. Technol.* **6** 133
[7] Russell D and Weinreb S 2012 *IEEE Trans. THz Sci. Technol.* **60** 1641
[8] Weinreb S, Bardin J, Mani H and Jones G 2009 *Rev. Sci. Instrum.* **80** 044702
[9] Bardin J C 2021 *IEEE Solid-State Circuits Magazine* **13** 22
[10] Weinreb S, Bardin J C and Mani H 2021 *IEEE Trans. Microwave Theory Tech.* **55** 2306
[11] Bardin J C and Weinreb S 2008 *IEEE MTT-S International Microwave Symposium Digest,* June 15–20, 2008 Atlanta, GA, USA, p. 459
[12] Niu G, Cressler J D, Zhang S, Ansley W E, Webster C S and Harame D L 2001 *IEEE Trans. Electron Dev.* **48** 2568
[13] Yau K H K, Chevalier P, Chantre A and Voinigescu S P 2011 *IEEE Trans. Microwave Theory Tech.* **59** 1983
[14] Bardin J C 2009 *Silicon-Germanium Heterojunction Bipolar Transistors for Extremely Low-Noise Applications*, Ph. D. Dissertation (Pasadena: California Institute of Technology)
[15] Fernandez J E 1998 *TMO Progress Report* **15** 42
[16] Sheldon A, Belostotski L, Mani H, Groppi C E and Warnick K F 2021 *IEEE Microwave Magazine* **22** 52
[17] Bardin J C and Weinreb S 2009 *IEEE Microwave and Wireless Components Letters* **19** 2020041
[18] Chang S W and Bardin J C 2017 *IEEE MTT-S International Microwave Symposium*, June 04–09, 2017 Honolulu, HI, USA, p. 157
[19] Hosseini, Mohsen, Wong W T and Bardin J C *IEEE MTT-S International Microwave Symposium*, June 02–07, 2019 Boston, MA, USA, p. 164